

**PS Stratigraphic Architecture of a Structurally Confined, Ponded Submarine Fan: An Outcrop Study of the Guaso I Turbidite System (Ainsa Basin, Southern Spanish Pyrenees)\***

**Gregory Gordon<sup>1</sup>, David Pyles<sup>2</sup>, Julian Clark<sup>3</sup>, Matthew Hoffman<sup>4</sup>, Jane Stammer<sup>2</sup>, Jeremiah D. Moody<sup>2</sup>, and Grace Ford<sup>2</sup>**

Search and Discovery Article #50431 (2011)

Posted June 30, 2011

\*Adapted from poster presentation at AAPG Annual Convention and Exhibition, Houston, Texas, USA, April 10-13, 2011

<sup>1</sup>Dept. of Geology and Geol. Engineering, Chevron Center of Research Excellence at the Colorado School of Mines, Golden, CO ([ggordon@mines.edu](mailto:ggordon@mines.edu))

<sup>2</sup>Dept. of Geology and Geol. Engineering, Chevron Center of Research Excellence at the Colorado School of Mines, Golden, CO

<sup>3</sup>Chevron ETC, San Ramon, CA

<sup>4</sup>Chevron Gulf of Mexico Business Unit, Covington, LA

**Abstract**

Ponded, structurally confined submarine fan systems are common features near earth's continental margins. These systems often form significant hydrocarbon reservoirs, and they can occur in a wide variety of tectonic settings, including salt-withdrawal mini-basins, extensional-contractional systems (e.g., Mississippi fan fold-belt, and offshore Nigeria), transtensional regions, foreland basins, and fore-arc basins. The Eocene Guaso turbidite system crops out in the Ainsa Basin, a piggyback basin within the South Pyrenean foreland basin system. Outcrops of the Guaso I (GI), a fourth-order cycle within the Guaso turbidite system, reveal a structurally confined, distributive submarine fan.

GI outcrops provide a rare opportunity to document stratigraphic architecture, as well as proximal-to-distal changes in gross thickness, net-sand thickness, lithofacies associations, and reservoir quality for a structurally confined submarine fan. The strata in the proximal slope depositional setting are dominated by mass-transport-deposits (MTDs), sandy debrites, mud-filled channels, and occasional pebble- or sandstone-filled channels. Net-sand values are relatively low (< 10 m) in this area, and gross thickness increases downslope. The medial slope setting contains bedded mudstones, as well as sandstone-filled channels and levees. Net-sand and gross thickness values are higher than in the proximal slope setting. Near the basin's depocenter, the GI is comprised of mudstone overlain by a thin MTD, which is in turn overlain by ~ 80 m of vertically connected sandstone (with some minor siltstones). The vertical succession of this dominantly sandstone package is: (1) basal lobes; (2) distributary channels and lobes; (3) interbedded very-fine-sandstones and siltstones. This region has the highest net-sand and gross thickness (~ 150 m) values of the entire system. Near the distal and lateral fan margins, there are minor sandstone-filled channels and thin, tabular sandstone beds intercalated with laminated mudstone. This depositional region has the lowest net-sand values (1-3 m) of the entire GI system.

Stratigraphic stacking patterns document that the GI fan increased in depositional area through time. As depositional area increased, successive lobes and channels increased in the degree of compensational stacking. Data collected in this study can be used to predict architectural and facies patterns in ponded strata of structurally confined turbidite systems in the subsurface.

### **Selected References**

Beaubouef, R.T., and S.J. Friedmann, 2000, High resolution seismic/sequence stratigraphic framework for the evolution of the Pleistocene intra slope basins, western Gulf of Mexico; depositional models and reservoir analogs, *in* P. Weimer, R.M. Slatt, J. Coleman, N.C. Rosen, C.H. Nelson, A.H. Bouma, M.J. Styzen, and D.T. Lawrence, (eds.), Deep-water reservoirs of the world: Proceedings of the 20<sup>th</sup> Annual Bob F. Perkins Research Conference, Gulf Coast Section SEPM Foundation, p. 40-60.

Booth, J.R., M.C. Dean, A.E. DuVernay III, and M.J. Styzen, 2003, Paleo-bathymetric controls on the stratigraphic architecture and reservoir development of confined fans in the Auger Basin; central Gulf of Mexico slope: *Marine and Petroleum Geology*, v. 20/6-8, p. 563-586.

Clark, J., D. Pyles, R. Bouroullec, R. Amerman, M. Hoffman, J.D. Moody, A. Moss-Russell, P. Setiawan, H. Silalahi, T. Heard, C. Guzowski, A. Fildani, N. Drinkwater, and M. Pyrcz, 2010, Structural Controls on Deepwater Architecture and Facies in the Eocene Ainsa Basin, Spanish Pyrenees: AAPG Annual Convention April, 2010, New Orleans, Louisiana.

Fernandez, O., J.A. Munoz, P. Arbues, O. Falivene, and M. Marzo, 2004, Three-dimensional reconstruction of geological surfaces: An example of growth strata and turbidite systems from the Ainsa basin (Pyrenees, Spain): *AAPG Bulletin*, v. 88/8, p. 1049-1068.

Hoffman, M., 2009, Tectono-Stratigraphic Analysis of a Deep-Water Growth Basin, Ainsa Basin, Northern Spain: Colorado School of Mines, Master's thesis in preparation, 203 p.

Madof, A.S., N. Christie-Blick, and M.H. Anders, 2009, Stratigraphic controls on a salt-withdrawal intraslope minibasin, north-central Green Canyon, Gulf of Mexico; implications for misinterpreting sea level change: *AAPG Bulletin*, v. 93/4, p. 535-561.

Moody J.D., D. Pyles, R. Bouroullec, J. Clark, M. Hoffman, P. Setiawan, 2010, The Eocene Morillo Turbidite System (South-Central Pyrenees, Spain): Helping to Reduce Uncertainty of Sub-Surface Data Interpretation in a Deep Marine Growth Basin: AAPG Annual Convention, New Orleans, Louisiana, Abstracts, Search and Discovery abstract set #90104, Web accessed 16 June 2011, [http://www.searchanddiscovery.com/abstracts/pdf/2010/annual/abstracts/ndx\\_moody.pdf](http://www.searchanddiscovery.com/abstracts/pdf/2010/annual/abstracts/ndx_moody.pdf)

Muñoz, J.A., P. Arbues, and J. Serra-Kiel, 1998, The Ainsa Basin and the Sobrarbe oblique thrust system: Sedimentological and tectonic processes controlling slope and platform sequences deposited synchronously with a submarine emergent thrust system, *in* A.M. Hevia, and A.R. Soria, (eds.), Field Trip Guidebook of the 15th International Sedimentological Congress, Alicante, p. 213-223.

Pickering, K.T. and N.J. Bayliss, 2009, Deconvolving tectono-climatic signals in deep-marine siliciclastics, Eocene Ainsa Basin, Spanish Pyrenees; seesaw tectonics versus eustasy: *Geology*, v. 37/3, p. 203-206.

Pyles, D.R., 2007, Architectural elements in a ponded submarine fan, Carboniferous Ross Sandstone, western Ireland, *in* T. H. Nilsen, R.D. Shew, G.S. Steffens, and J.R.J. Studlick, Atlas of Deepwater Outcrops: AAPG Studies in Geology 56, CD-ROM, 19 p.

D.R. Pyles, A. Moss-Russell, H. Silalahi, D. A. Anderson, B. Bracken, J. Clark, R. Bouroullec, J.D. Moody, 2010, Integrating Outcrop Data to Define Regional and Reservoir-Scale Patterns in Prograding Shelf-Slope-Basin Systems, Sobrarbe Formation, Spain: AAPG Annual Convention, New Orleans, Louisiana, Abstracts, Search and Discovery abstract set #90104, Web accessed 16 June 2011, [http://www.searchanddiscovery.com/abstracts/pdf/2010/annual/abstracts/ndx\\_pyles.pdf](http://www.searchanddiscovery.com/abstracts/pdf/2010/annual/abstracts/ndx_pyles.pdf)

Setiawan, P., R. Bouroullec, D.R. Pyles, J. Clark, M. Hoffman, and J.D. Moody, 2009, Facies Distribution and Stratigraphic Architecture along Growing Basin Margins, Eocene Deepwater Morillo Depositional System, Ainsa Basin, Spain: AAPG Annual Convention, Denver, Colorado, Abstracts, Search and Discovery abstract set #90090, Web accessed 16 June 2011 (<http://www.searchanddiscovery.net/abstracts/html/2009/annual/abstracts/setiawan.htm>)

Smith, M.A., and W.W. Shedd, 2004, Effects of gas hydrate on seafloor and borehole stability in the deepwater Gulf of Mexico; seismic prediction and drilling results: AAPG Annual Meeting, Dallas, Texas, Abstracts, Search and Discovery abstract set #90026, Web accessed 23 June 2011, <http://www.searchanddiscovery.com/abstracts/html/2004/annual/abstracts/Smith06.htm>

Sutcliffe, C., and K.T. Pickering, 2009, End-signature of deep-marine basin-fill, as a structurally confined low-gradient clastic slope: The Middle Eocene Guaso system, south-central Spanish Pyrenees: *Sedimentology*, v. 56/6, p. 1670-1689.

Winker, C.D., and J.R. Booth, 2000, Sedimentary dynamics of the salt-dominated continental slope, Gulf of Mexico: integration of observations from the seafloor, near-surface, and deep subsurface. Deep-Water Reservoirs of the World: Proceedings of the GCSSEPM 20th Annual Research Conference, p. 1059-1086.





# Stratigraphic Architecture of a Structurally Confined, Ponded Submarine Fan: An Outcrop Study of the Guaso I Turbidite System (Ainsa Basin, Southern Spanish Pyrenees)



Gregory Gordon<sup>1</sup> [ggordon@myemail.mines.edu](mailto:ggordon@myemail.mines.edu), David Pyles<sup>1</sup>, Julian Clark<sup>2</sup>, Matt Hoffman<sup>3</sup>, Jane Stammer<sup>1</sup>, Jeremiah Moody<sup>1</sup>, Grace Ford<sup>1</sup>

<sup>1</sup> Chevron Center of Research Excellence, Department of Geology and Geological Engineering, Colorado School of Mines, Golden, Colorado

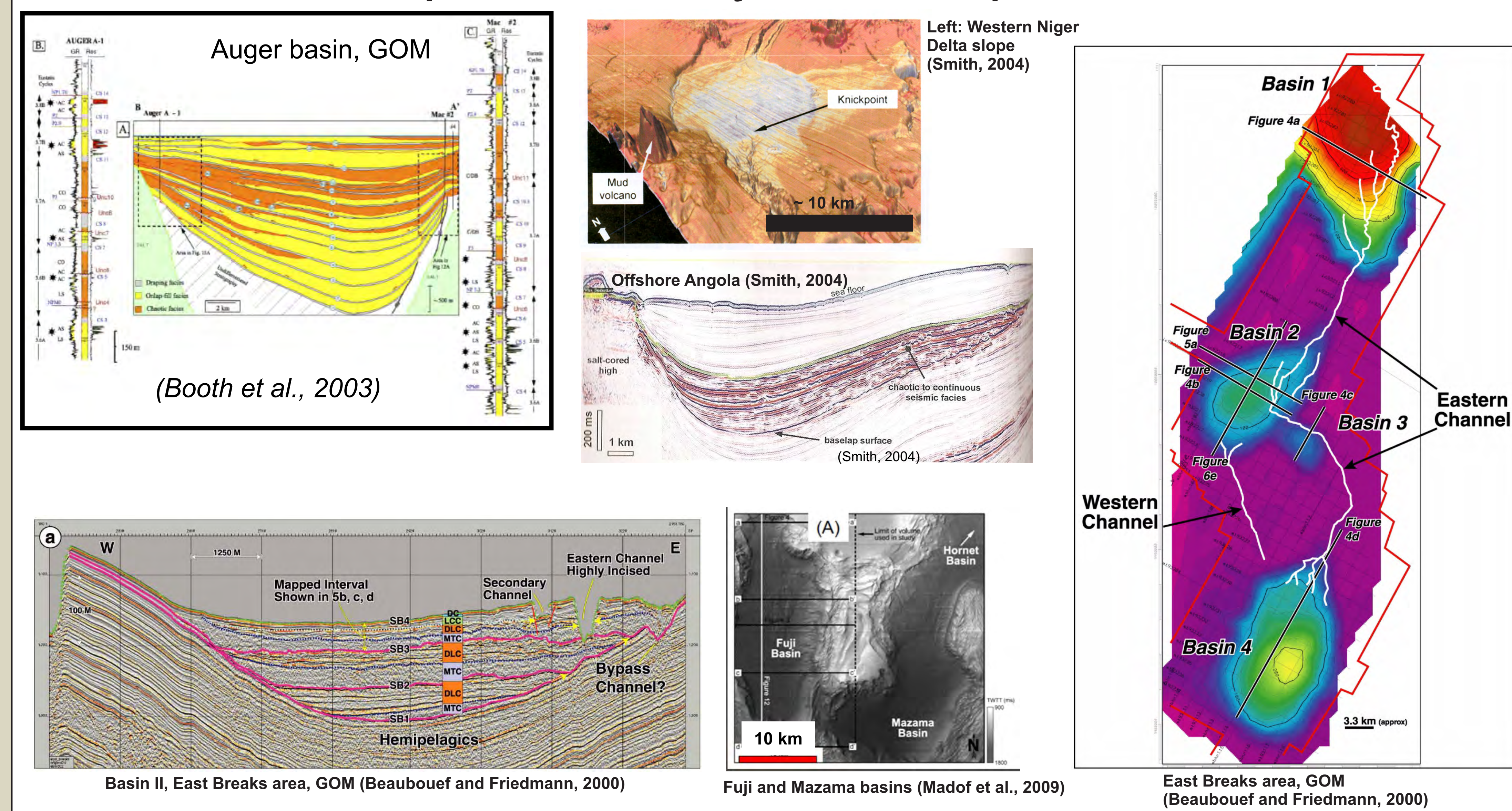
<sup>2</sup> Chevron Energy Technology Company, San Ramon, California

<sup>3</sup> Chevron Gulf of Mexico Business Unit, Louisiana

## Introduction

- Structurally confined turbidite systems are prolific hydrocarbon reservoirs around the world, from the Gulf of Mexico to southern California to offshore West Africa.
- These reservoirs are most commonly characterized with seismic, well, and/or conventional core data. Each of these datasets, however, has limitations in either detail or spatial extent.
- Detailed stratigraphic field studies in analogous deepwater basins, such as the Ainsa basin, will yield critical quantitative data regarding styles of longitudinal, lateral, and temporal variations in reservoir architecture.

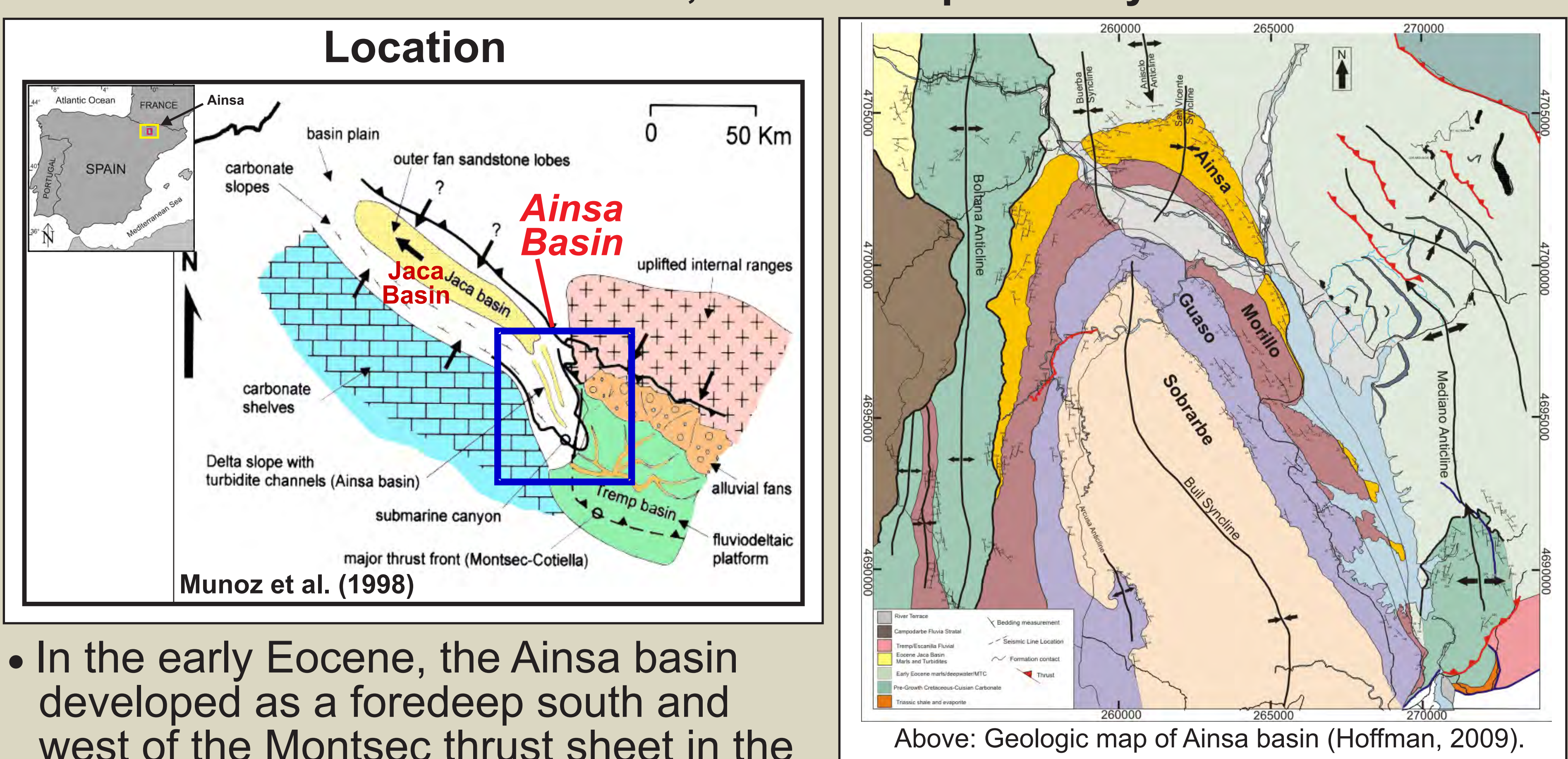
### Examples of structurally confined deepwater basins:



## Data/methods

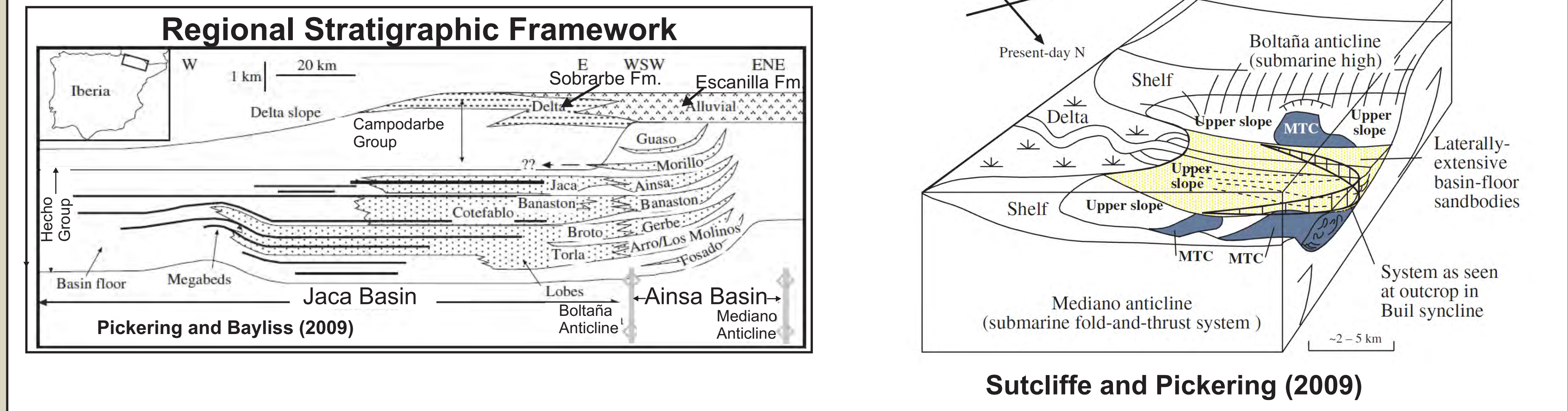
- Field mapping of cycle-bounding condensed sections, sandstone bodies, and mass-transport-deposits (MTDs, i.e. slumps, slides, debris-flow deposits) was conducted.
- We define *cycles* based on condensed sections, not speculative sequence boundaries.
- Measured 30 sections (1,980 m total); 429 paleocurrent measurements in the Guaso I.
- We observed four principal architectural elements and 14 facies types.
- We correlated measured sections, and interpreted time-significant surfaces within the Guaso I cycle. We used these correlations to construct stratigraphic cross-sections.
- We used the thickness and net-sandstone values to create isopach maps (gross-thickness and net-sandstone).
- Paleogeographic reconstruction using above correlations and paleocurrent data.

### Ainsa basin, southern Spanish Pyrenees



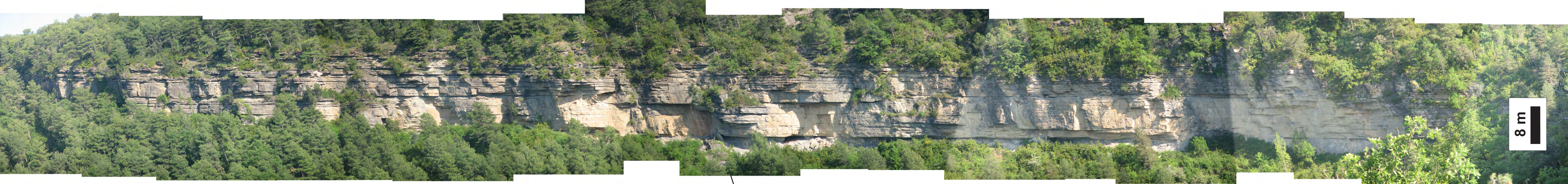
- In the early Eocene, the Ainsa basin developed as a foredeep south and west of the Montsec thrust sheet in the South Pyrenean foreland basin system (Fernandez et al., 2004).
- As thrusting propagated toward the foreland in the middle Eocene, the Ainsa basin evolved into a piggyback basin (Fernandez et al., 2004; Hoffman, 2009).
- The entire Guaso system was deposited in ~ 800 ka (Pickering and Bayliss, 2009).

### Previous Work

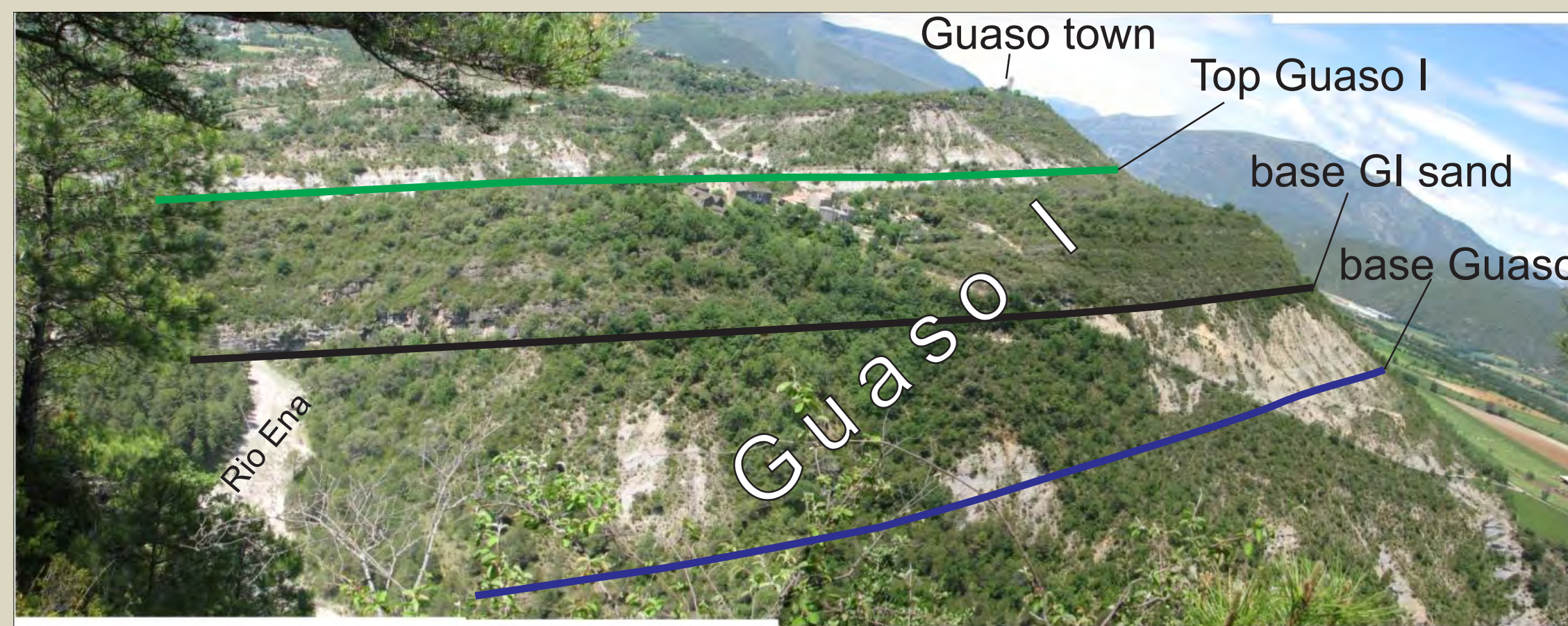


- Sutcliffe and Pickering (2009) interpreted the Guaso as a structurally confined, delta-fed, low-gradient deepwater clastic depositional system.
- Pickering and Bayliss (2009) interpreted that the Guaso system was sourced from the south, between the two growth anticlines.
- In our present study, we offer a different interpretation for the Guaso (specifically, Guaso I) turbidite system.

## Geologic Setting



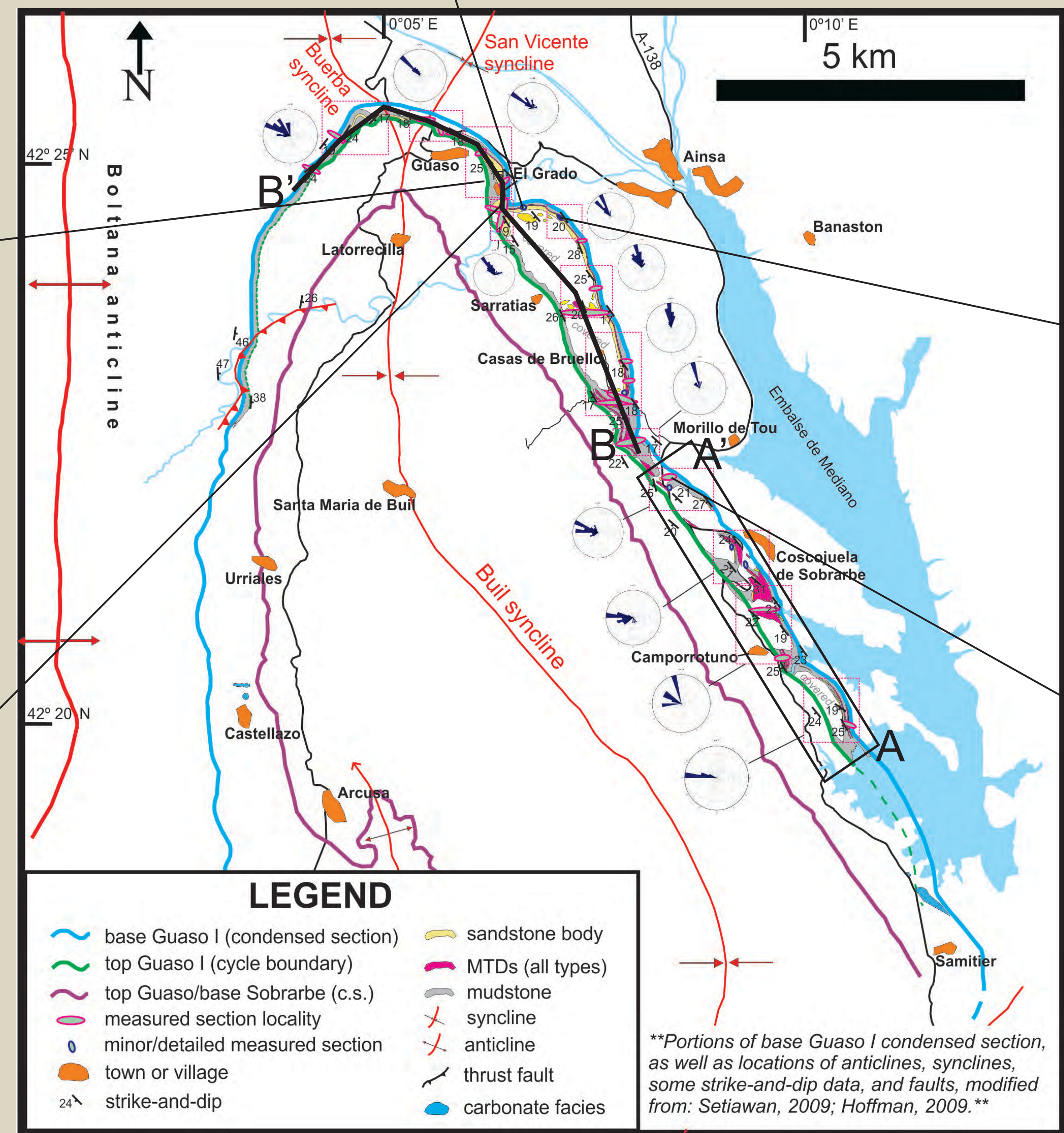
•Above: Proximal lobe elements near Rio Ena. There are tabular beds, as well as beds and bedsets that thicken, thin, and exhibit erosional relief. View is looking south.



•Above: View looking northwest toward El Grado village and Guaso town.



•Above: Lobe complex exposed at Rio Ena. View looking ~ west-northwest.

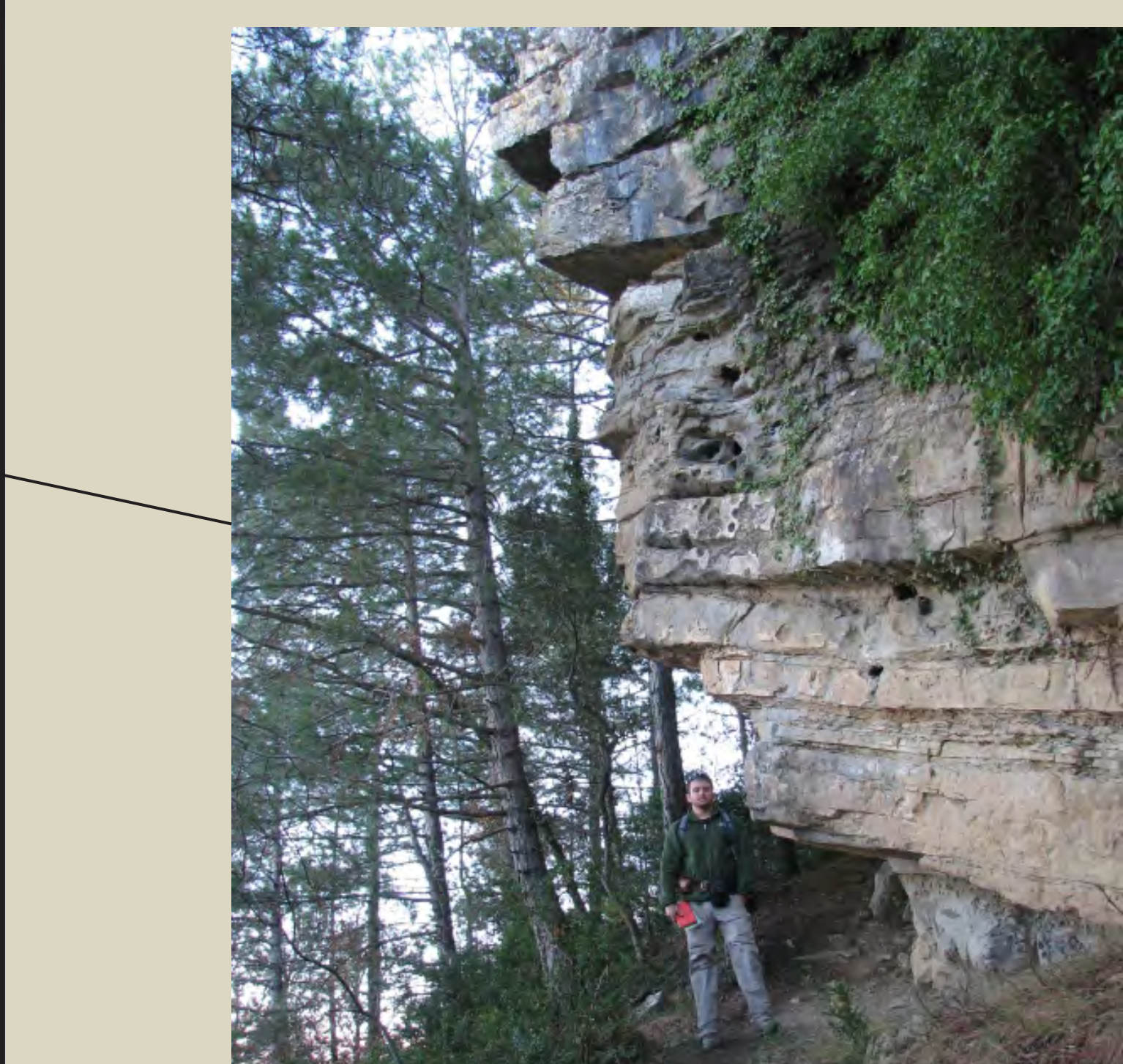


### Geologic map of Guaso system

- The Ainsa basin is currently expressed as the Bui syncline.
- This basin is bounded by the Mediano and Boltana anticlines, to the east and west, respectively. These structures were active in the middle Eocene during the deposition of the basin's deepwater clastic systems.
- The Guaso I turbidite sandstone outcrops are mostly located along the basin's east flank.

• Left: Outcrop exposure at "Waterfall Canyon" along Rio Ena. See measured section in cross-section B-B'. (Note person for scale.)

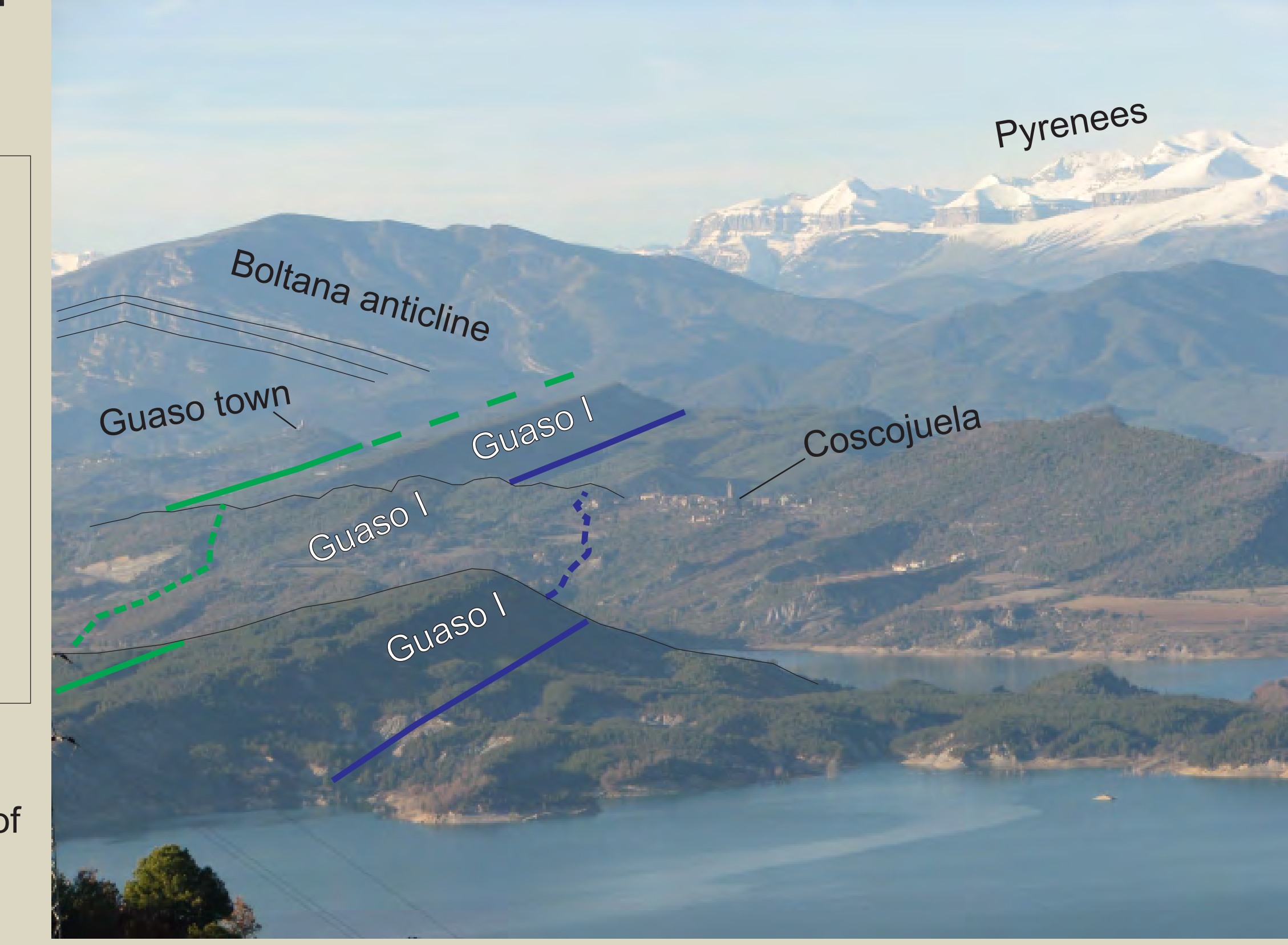
• Right: View looking northwest, along strike of Guaso system.



• Left: Tabular Guaso I beds at Osqueta da Calura trail marker, east of the Rio Ena outcrop. These beds are the most proximal lobe deposits. Note field geologist for scale.

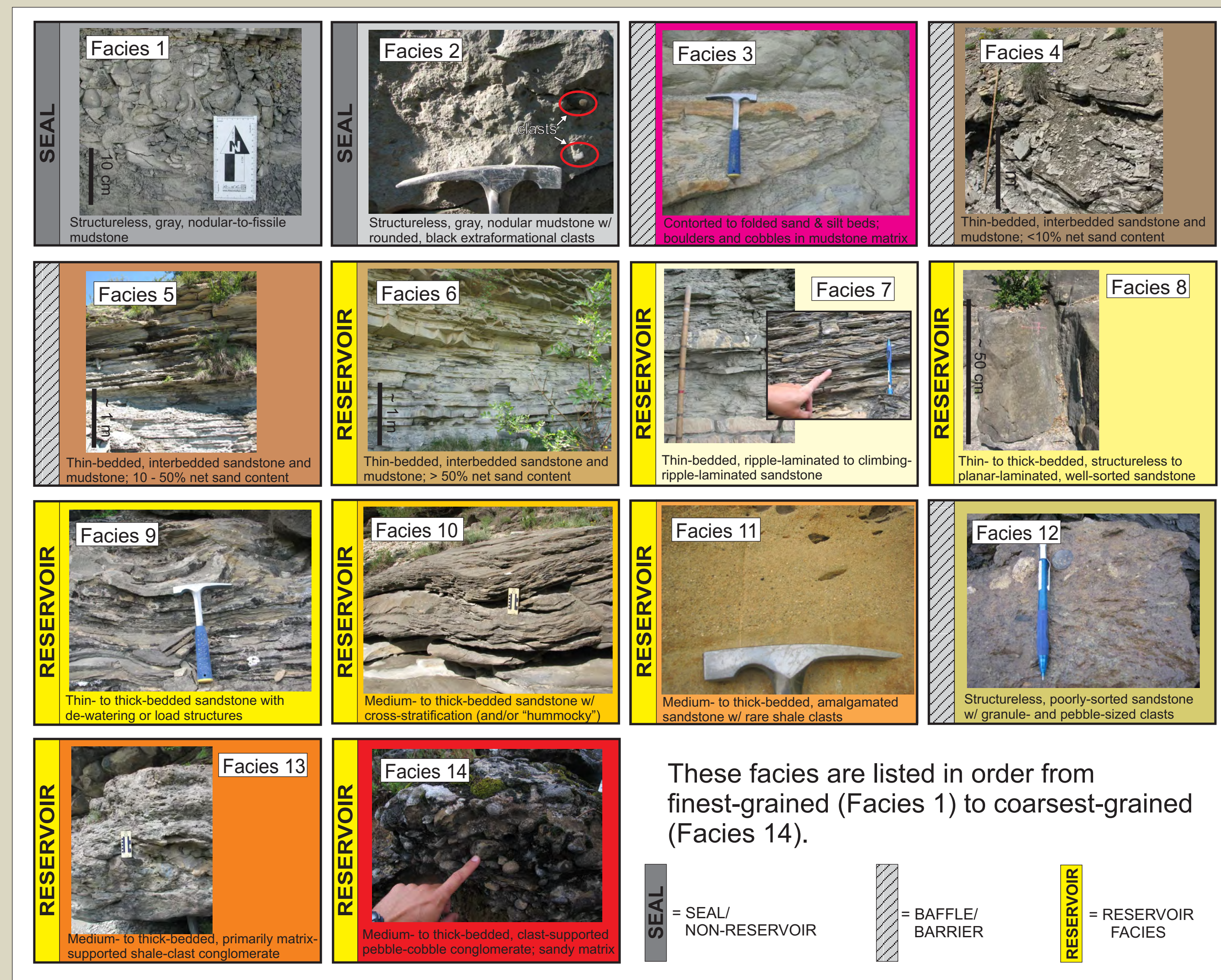


• Below: Slope channel complex exposed immediately east of Highway A-138. See Page 2 for an annotated interpretation of this channel complex.





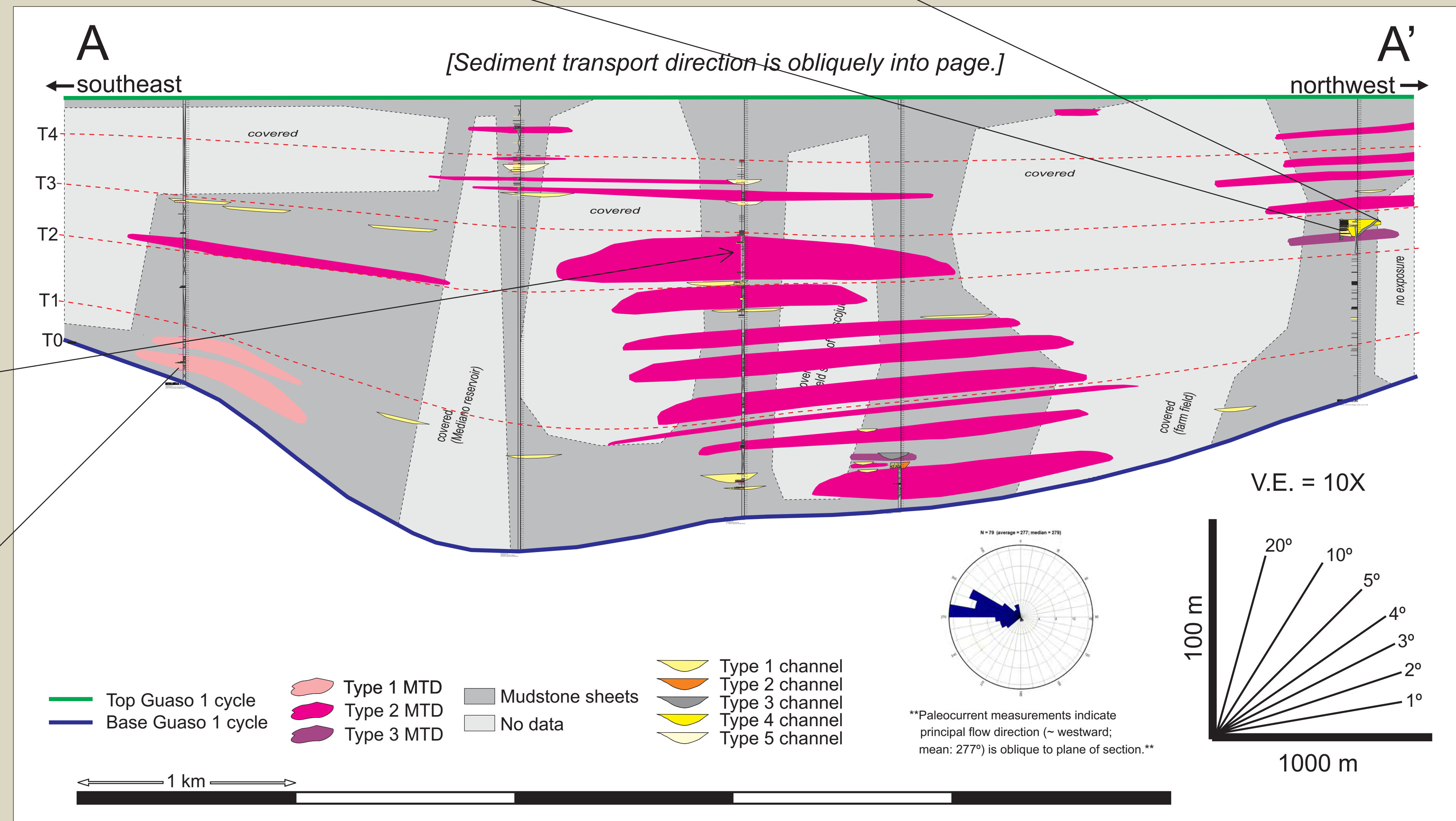
## Facies



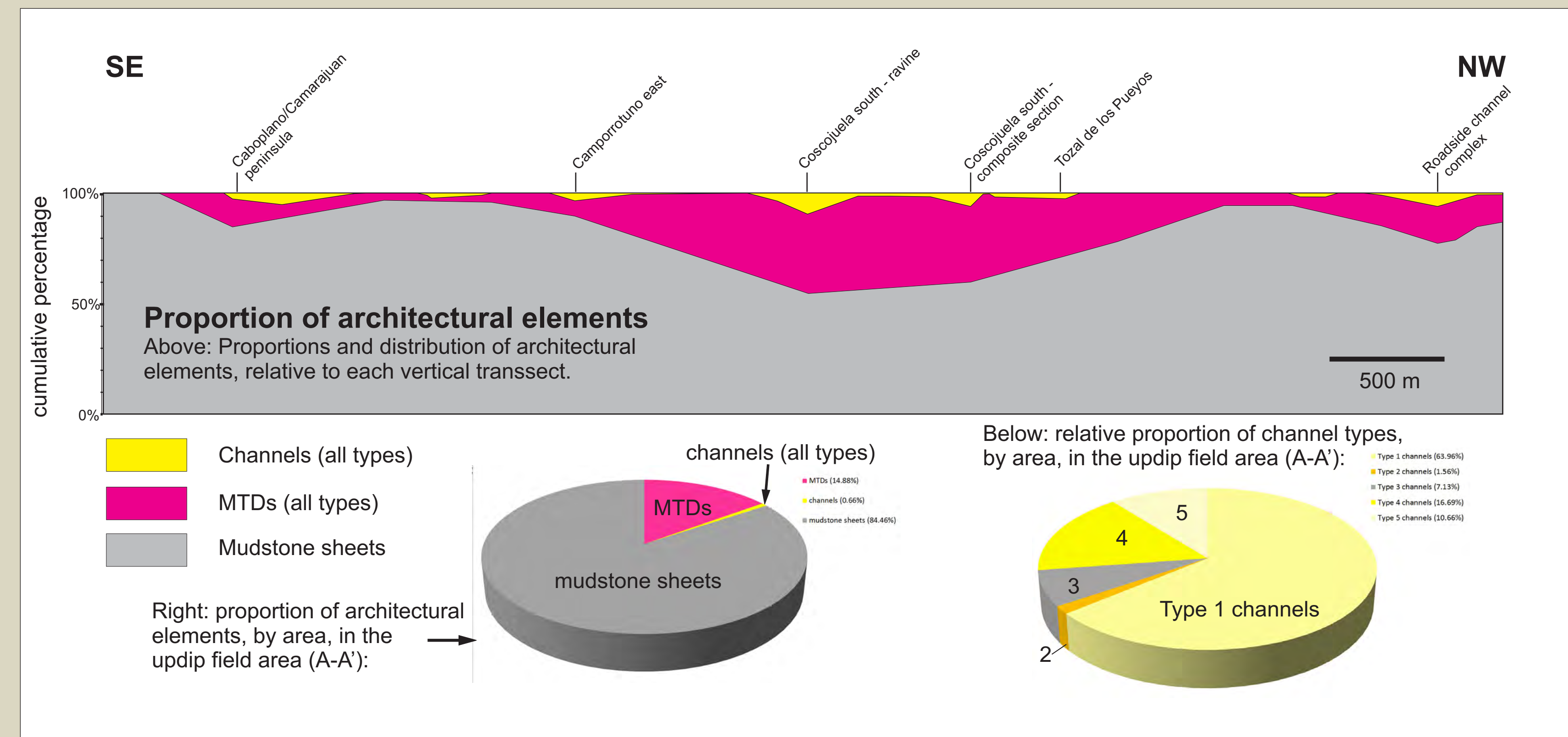
| Facies | Reservoir facies? | Description   | Model grain size(s)              | Net-sand content (%) | Interpreted sediment support mechanism         | Interpreted depositional process   | Interpreted flow type                            | Relative sediment concentration during transport |
|--------|-------------------|---|----------------------------------|----------------------|--|--|--|--|
| 1      |                   | Structureless, gray, nodular-to-fine mudstone   | clay                             | 0                    | frictional settling; possible fluid turbulence | suspension   | hypopycnal plume; fine-grained turbidity current | low  |
| 2      |                   | Structureless, gray, nodular mudstone w/ black and dark gray clasts (granule- or pebble-sized of clay, mudstone, and carbonate mudstone matrix comprises >95% of this facies)   | clay (clasts)                    | 0                    | matrix strength                                | frictional freezing, cohesive freezing   | debris-flow                                      | high   |
| 3      |                   | Contorted to folded sandstone, siltstone, and claystone beds; turbidite sandstone and silty sandstone and boulders variably distributed in the mudstone matrix  | fine silt sand                   | 0*                   | matrix strength                                | frictional freezing, cohesive freezing   | slump, slides (area, Marston and Bakken, 1995)   | high   |
| 4      |                   | Thin-bedded, interbedded sandstone and mudstone; <10% net sand content  | fine silt sand                   | <10                  | fluid turbulence                               | suspension and traction sedimentation  | turbidity current                                | low  |
| 5      |                   | Thin-bedded, interbedded sandstone and mudstone; 10-50% net sand content  | fine silt sand                   | 10-50                | fluid turbulence                               | suspension and traction sedimentation  | turbidity current                                | low  |
| 6      |                   | Thin-bedded, interbedded sandstone and mudstone; >50% net sand content  | fine and medium sand (fine silt) | >50                  | fluid turbulence                               | suspension and traction sedimentation  | turbidity current                                | low  |
| 7      |                   | Thin-bedded, ripple-laminated to climbing-ripple laminated sandstone  | very fine sand                   | >90                  | fluid turbulence                               | traction sedimentation (lower-flow regime)   | turbidity current                                | low  |
| 8      |                   | Thin to thick-bedded, structureless to planar laminated, well-sorted sandstone, amalgamation surfaces can be present  | fine sand                        | 100                  | fluid turbulence                               | suspension (structureless); traction (planar laminated)                                    | turbidity current                                | low  |
| 9      |                   | Thin to thick-bedded sandstone with dewatering or load structures (thrust structures, contorted bedding, etc.)  | fine sand                        | >90                  | fluid turbulence                               | initial suspension or traction sedimentation, followed by dewatering or loading from above | turbidity current                                | low  |
| 10     |                   | Medium to thick-bedded sandstone with large-scale cross-stratification (broadly bedform control)  | fine sand                        | >95                  | fluid turbulence                               | traction sedimentation, w/ some deposition due to suspension failure                       | turbidity current                                | low  |
| 11     |                   | Medium to thick-bedded, amalgamated sandstone w/ horizontally aligned shale clasts (oblique pediments); normal grading common, as well as common fluid flow of both structures; poorly sorted sandstone w/ large grains and pebbles (well-sorted clasts 1-5% clasts are rounded sandstone and silt-sandstone) | medium sand (clasts pebbles)     | 95                   | fluid turbulence                               | turbidity current  | low-medium                                       |  |
| 12     |                   | Medium to thick-bedded, primarily matrix-supported shale clast conglomerate (shale clasts are elongate pebbles and compose <40%); matrix is medium sand   | medium sand (clasts pebbles)     | 96                   | matrix strength                                | frictional freezing, cohesive freezing   | debris-flow, or possibly a "hybrid" flow         | high   |
| 13     |                   | Medium to thick-bedded, pebble-cobble conglomerate in sandy matrix (pebbles clasts are rounded sandstone and sandstone; the facies traces into underlying contorted mudstone facies)  | medium sand (clasts pebbles)     | 60                   | dispersive pressure and fluid turbulence       | traction sedimentation   | turbidity current (high concentration?)          | high   |
| 14     |                   |   |                                  |                      |  |  |  |  |

Left: location of cross-section A-A'

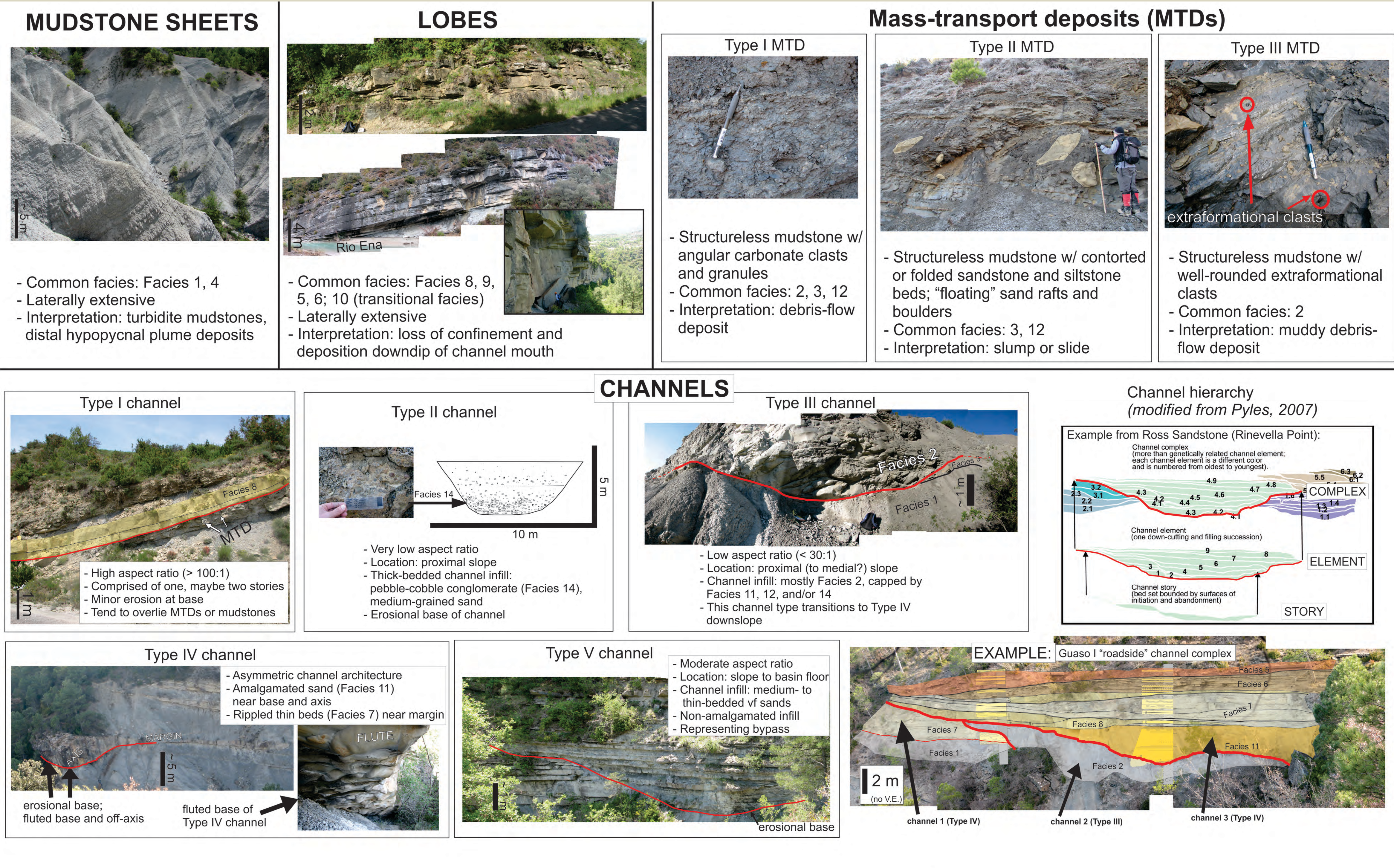
## Cross-section A-A'



- Cross-section A-A' and accompanying paleocurrent data indicate that this area was the entry point for Guaso I sediments, which were transported from east to west.
- These sediments were then deposited on the basin floor to the northwest.
- This area contains abundant MTDs and Type 1 channel elements.
- MTDs are thickest in the axis of this feeder system.

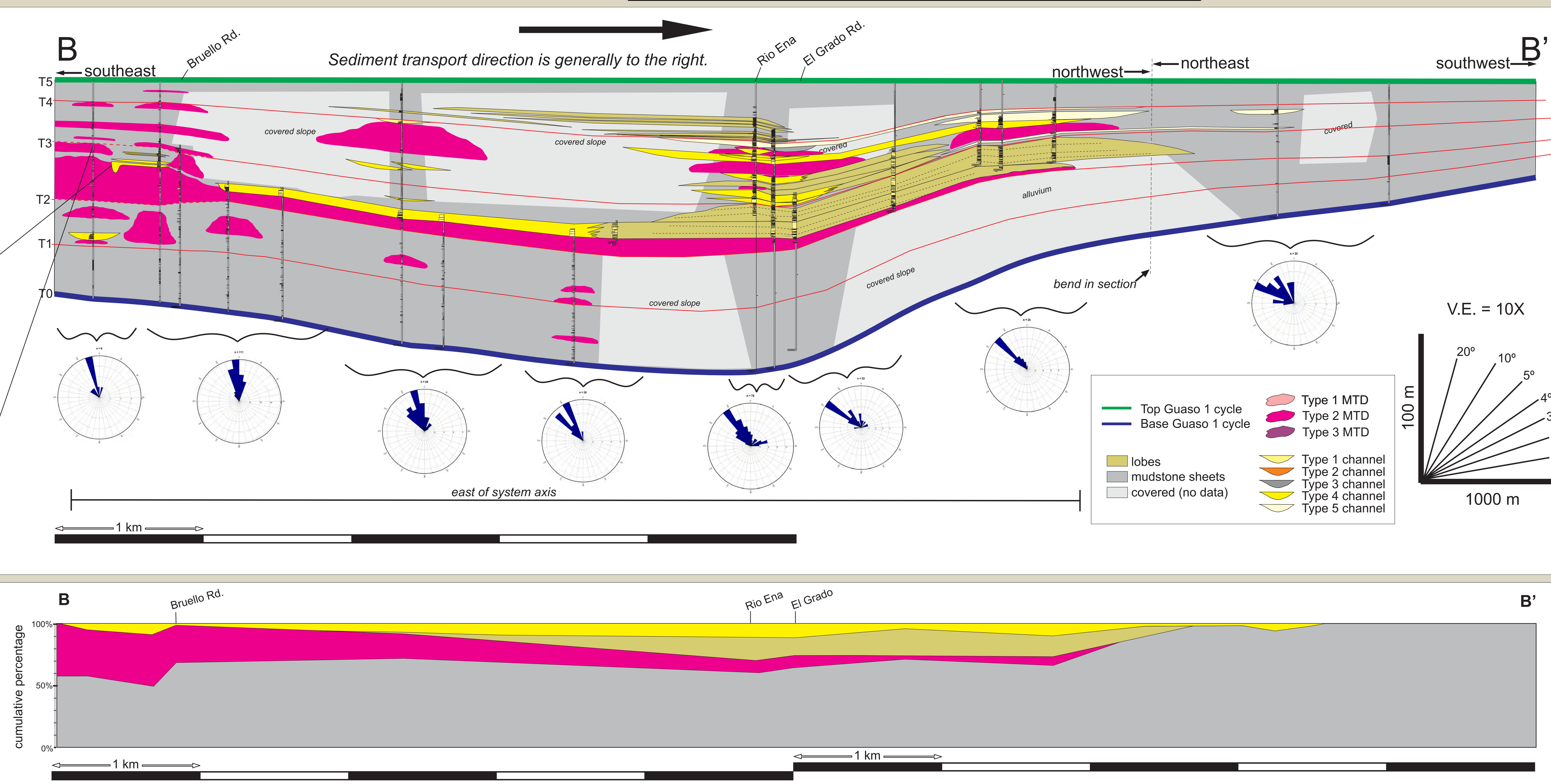


## Architectural elements

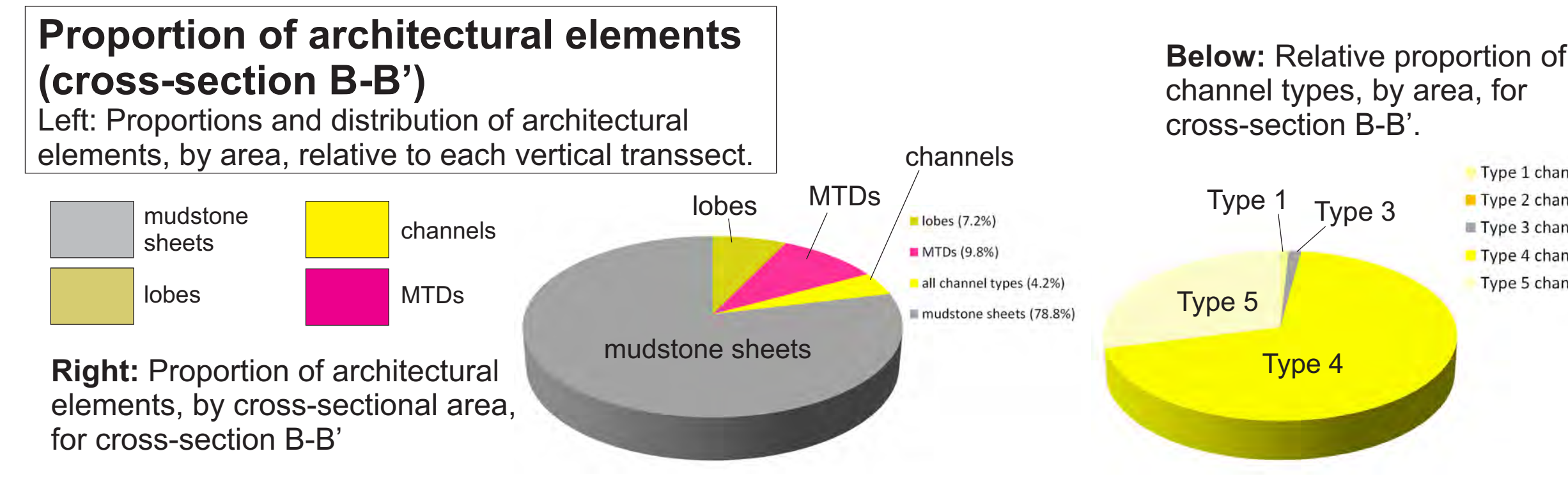


Left: location of cross-section B-B'

## Cross-section B-B'

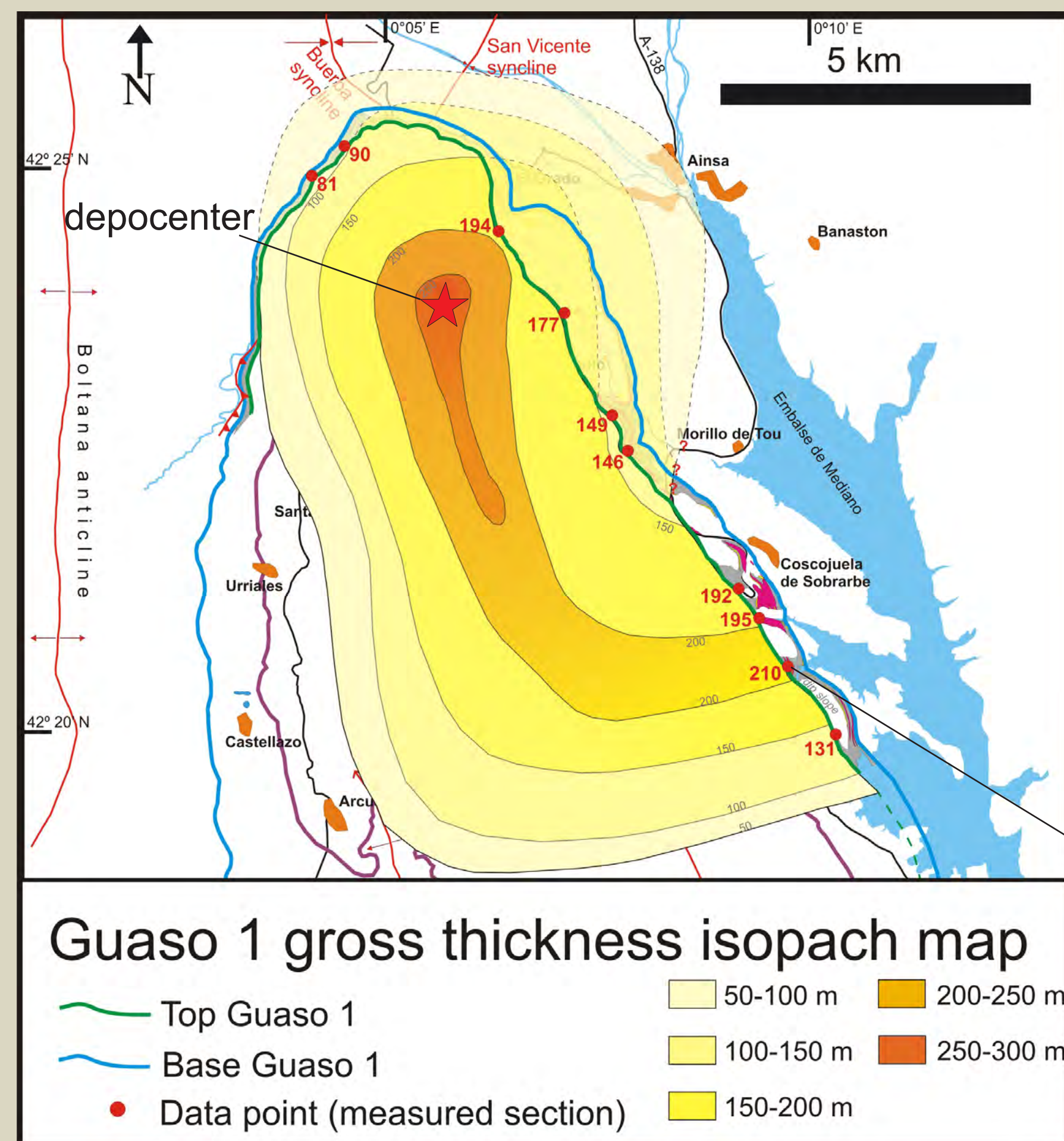


- MTDs are abundant in the southeast part of cross-section B-B'; they decrease in abundance to the northwest (downslope).
- Lobes generally increase in abundance to the northwest; they are most abundant near the depocenter. Beyond the depocenter, the abundance of lobes decreases.
- The Type 4 channel overlying the MTD immediately above surface T2 is present in continuous outcrop for ~3 km. (Paleocurrents are generally parallel to strike.) This channel feeds the basal lobes at Rio Ena.
- This cross-section seems to suggest that there are no Guaso I sand bodies near the depocenter below surface T2. However, paleocurrent data and stratigraphic relationships illustrated in cross-section A-A' suggest that B-B' is an off-axis cross-sectional slice; it is inferred here that there are sandy Guaso I lobes in a more axial position (to the southwest).
- 37.6% of the area of cross-section B-B' is covered or removed by erosion.

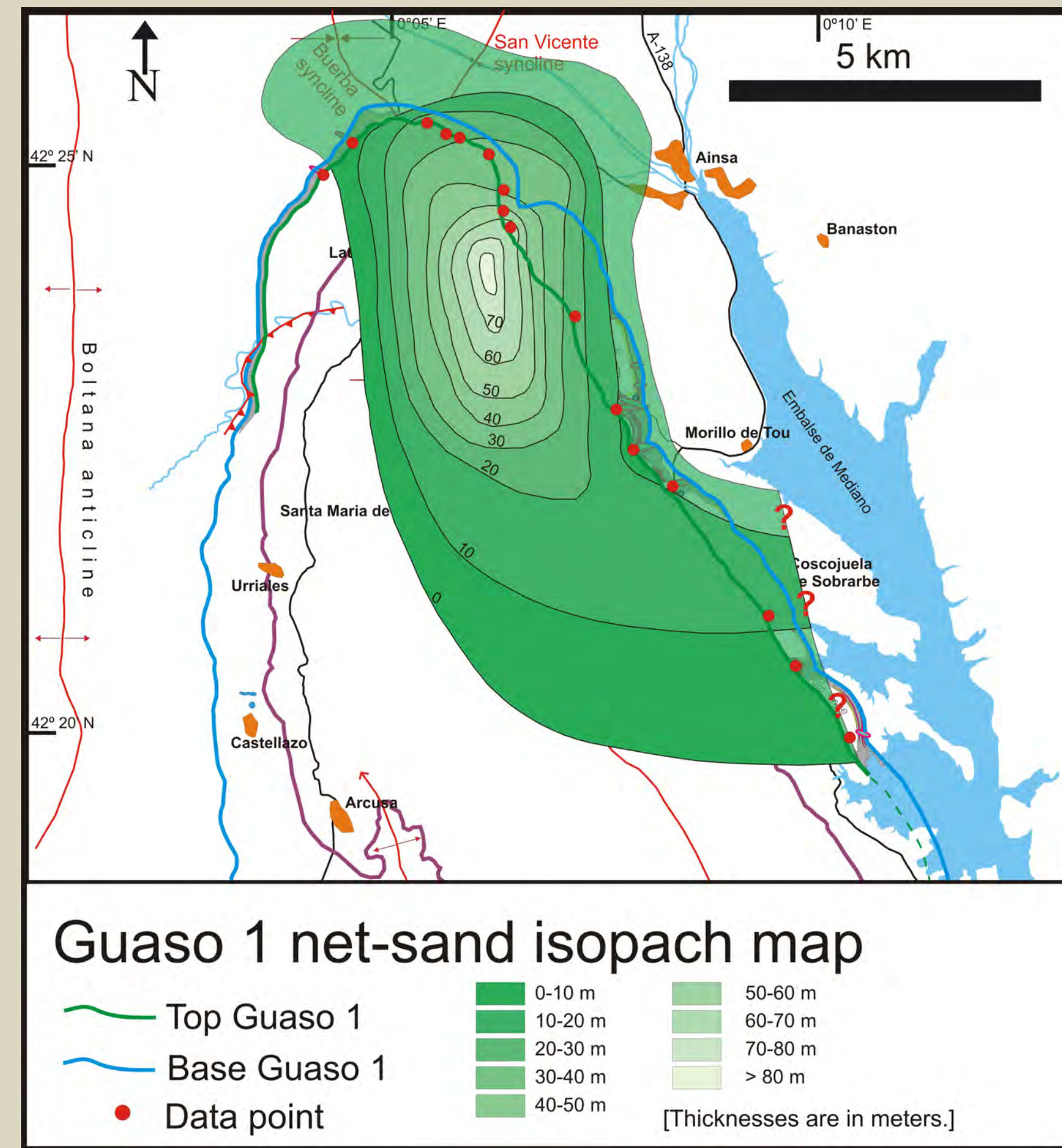




## Isopach Maps



- Measured sections and correlation panels yielded stratigraphic values which were used to create gross-thickness and net-sandstone isopach maps.
- We offer a complete subsurface interpretation of the Guaso I system, constrained by outcrop data.
- The Guaso I system is thickest in the subsurface, ~ 2 km southwest of the Rio Ena locality. This is defined as the depocenter.
- The Guaso I is also very thick on the slope (at outcrops immediately east of Camporrotuno) – in the updip “feeder area” of the system.



- The Guaso I system has the highest net-sandstone values near the depocenter (located southwest of the Rio Ena locality).
- This trend is indicative of out-of-grade systems (*sensu* Pyles et al., 2010), e.g. Ross sandstone and Annot sandstone.
- High net-sandstone content is present in areas dominated by deposition of lobes and distributary channels.
- Paleocurrent data, measured sections, and field mapping indicate that the Guaso I channels